# PAX2 Activates WNT4 Expression during Mammalian Kidney Development*

Elena Torban[‡], Alison Dziarmaga[§], Diana Iglesias[§], Lee Lee Chu[‡§], Tatiana Vassilieva[‡§], Melissa Little[¶], Michael Eccles[∥], Maria Discenza**, Jerry Pelletier**, and Paul Goodyer[‡§1]

From the [‡]Departments of Experimental Medicine and Pediatrics and the [§]Department of Human Genetics, McGill University, Montreal, Quebec, Canada, the [¶]Institute of Molecular Science, University of Queensland, Brisbane, Queensland, Australia, [∥]Developmental Genetics Laboratory, Department of Pathology, University of Otago, Dunedin, New Zealand, and the **Department of Biochemistry, McGill University, Montreal, Quebec H3G 1Y6, Canada

The transcription factor PAX2 is expressed during normal kidney development and is thought to influence outgrowth and branching of the ureteric bud. Mice with homozygous null *Pax2* mutations have developmental defects of the midbrain-hindbrain region, optic nerve, and ear and are anephric. During nephrogenesis, PAX2 is also expressed by mesenchymal cells as they cluster and reorganize to form proximal elements of each nephron, but the function of PAX2 in these cells is unknown. In this study we hypothesized that PAX2 activates expression of WNT4, a secreted glycoprotein known to be critical for successful nephrogenesis. PAX2 protein was identified in distal portions of the "S-shaped" body, and the protein persists in the emerging proximal tubules of murine fetal kidney. PAX2 activated *WNT4* promoter activity 5-fold in co-transfection assays with JTC12 cells derived from the proximal tubule. Inspection of the 5′-flanking sequence of the human *WNT4* gene identified three novel PAX2 recognition motifs; each exhibited specific PAX2 protein binding in electromobility shift assays. Two motifs were contained within a completely duplicated 0.66-kb cassette. Transfection of JTC12 cells with a *PAX2* expression vector was associated with a 7-fold increase in endogenous *WNT4* mRNA. In contrast, *Wnt4* mRNA was decreased by 60% in mesenchymal cell condensates of fetal kidney from mice with a heterozygous *Pax2* mutation. We speculated that a key function of PAX2 is to activate *WNT4* gene expression in metanephric mesenchymal cells as they differentiate to form elements of the renal tubules.

*PAX2* belongs to the "paired box" family of transcription factors. Like other family members, it is thought to orchestrate the patterns of gene expression in specific cells during organ development. Homozygous inactivation of the *Pax2* gene in mice causes malformation of the midbrain-hindbrain region, the optic nerve, and complete absence of the kidneys (1, 2). Although these observations clearly implicate PAX2 in the development of renal and neural tissue, little is known about its precise gene targets or the specific developmental processes in which it plays a role.

Studies thus far suggest that the developmental functions of PAX2 may be multiplex, activating distinct panels of genes in different cell lineages at different stages. During development of mammalian kidney,

PAX2 first appears during the caudal descent of the nephric duct where it affects the fate of a cell (3). When the nephric duct arrives at about somite 26, a "ureteric bud" (UB)[2] emerges from its wall and grows toward the adjacent lateral mesenchyme. This event is again orchestrated by PAX2 through activation of glial cell line-derived neurotropic Factor (GDNF) in the uninduced mesenchyme and activation of the GDNF receptor (RET) in UB cells (4). Thus, homozygous *Pax2* knockout mice lack normal ureteric bud outgrowth and are unable to induce metanephric kidneys (2).

A third function of PAX2 in developing kidney involves suppression of programmed cell death in ureteric bud cells. During normal development, the UB arborizes as it penetrates the metanephric mesenchyme, inducing nephrons to form at the tip of each branch. Final nephron endowment is determined by the extent of UB branching achieved at the point when new nephron formation comes to an end in the perinatal period. Mice and humans lacking one *Pax2* allele have increased apoptosis of UB cells, reduced UB branching, and suboptimal final nephron number (5, 6). Delivery of a pro-apoptotic gene (*Baxα*) to the developing UB reduces arborization (7); conversely, the branching defect seen in *Pax2* heterozygous mutants can be rescued by targeted expression of an anti-apoptotic gene (*Bcl2*) to the UB lineage[3] or by administration of caspase inhibitors to pregnant mice bearing heterozygous mutant *Pax2* fetuses (8).

Once within the mesenchyme, the arborizing UB delivers signals to nearby mesenchymal cells, inducing them to cluster at the tip of each UB branch. These induced mesenchymal cells express moderately high levels of PAX2 as they undergo a profound transformation into polarized epithelia, but the precise role of PAX2 during this process is unknown (2). Rapid cell division and coordinated cell movement result in twisting growth of an elongated "S-shaped" body with a central lumen lined by epithelial cells. Capillary ingrowth at one end allows formation of the glomerulus, and at its other end fusion with the UB branch tip affords outflow of luminal fluid into the common collecting system. Torban *et al.* (9) showed that PAX2 expression is associated with an increase in E-cadherin and suppression of vimentin levels in cultured fetal kidney cells, thus proposing that PAX2 might regulate the transition from mesenchyme to epithelium. However, the *PAX2* gene targets that might mediate this transition remain elusive.

In 1994, Stark *et al.* (10) reported that formation of S-shaped bodies in the developing kidney is critically dependent on WNT4, a member of the WNT family of secreted glycoproteins. WNT4 is expressed by the

[2] The abbreviations used are: UB, ureteric bud; RT, reverse transcriptase; Gapdh, glyceraldehyde-3-phosphate dehydrogenase; EMSA, electrophoretic mobility shift assay; DTT, dithiothreitol; PBS, phosphate-buffered saline; E, embryonic day; mut, mutant.
[3] E. Torban, A. Dziarmaga, D. Iglesias, L. L. Chu, T. Vassilieva, M. Little, M. Eccles, M. Discenza, J. Pelletier, and P. Goodyer, unpublished data.

induced metanephric mesenchymal cells as they cluster and undergo transformation into epithelia (10). Knock-out mice with homozygous inactivation of the *Wnt4* gene exhibit initial outgrowth of the ureteric bud, induction of mesenchymal cell clustering, and local expression of PAX2 but no further development of S-shaped bodies (10, 11). In the absence of S-shaped body formation, UB branching comes to an abrupt halt, and the mutant *Wnt4* mice are born anephric (10). In general, WNTs are thought to transmit signals to nearby cells bearing cognate receptors, thereby organizing cell alignment and tissue patterns during development (12). WNT4 was recently shown to be capable of activating the "canonical" $\beta$-catenin signaling pathway and therefore presumably regulates $\beta$-catenin-responsive gene targets, such as c-*Myc*, involved in cellular growth (13).

In this study, we hypothesize that a key function of PAX2 in the S-shaped body is to activate the *WNT4* gene. We show that PAX2 protein is present in the distal portion of the S-shaped body and persists in the emerging proximal tubular cells of fetal kidney. Transient transfection of a *PAX2* expression vector into JTC12 cells (derived from the simian proximal tubule) stimulates transcriptional activity of the human *WNT4* promoter. We identify several unique recognition motifs in the *WNT4* promoter that specifically bind PAX2 protein and show that JTC12 cells stably transfected with *PAX2* cDNA have increased endogenous WNT4 expression. Finally, we demonstrate that endogenous WNT4 expression is reduced in hypoplastic fetal kidneys of mice bearing a heterozygous *Pax2* mutation.

## MATERIALS AND METHODS

*Cell Lines, Transfections, and Luciferase Assays*—The monkey proximal tubule cell line (JTC12) was grown in Dulbecco's modified Eagle's medium supplemented with 10% heat-inactivated fetal bovine serum, 100 units/ml penicillin, 100 $\mu$g/ml streptomycin. Cells were incubated at 37 °C with 5% $CO_2$ in a humidified environment. The activity of a 10.7-kb *WNT4* promoter was analyzed in transient transfections of the JTC12 cell line in the presence or absence of a *PAX2* expression vector. Plasmid DNA preparation, cell culture, and transient transfections using FuGENE[TM] 6 transfection reagent (Roche Applied Science) were carried out as described (14), with modifications. Briefly, cells at 50–70% confluency were co-transfected with 0.4 $\mu$g of pRSV-$\beta$gal and 0.8 $\mu$g of human *WNT4* promoter/pGL2Basic. Cells were harvested 48 h after transfection, lysed in a passive lysis buffer (Promega), and assayed for firefly luciferase and normalized for $\beta$-galactosidase (Galacto-Star, Tropix). Transfections were performed in replicates of six on three separate occasions.

*Immunohistochemistry*—Immunohistochemisty for PAX2 was performed on 4% paraformaldehyde-fixed, paraffin-embedded embryonic mouse kidney tissues as described previously (6). Briefly, 7-$\mu$m sections were deparaffinized, rehydrated, and boiled twice for 5 min in 10 mM citrate buffer, pH 7.0. Endogenous peroxidase activity was quenched using 3% $H_2O_2$ in methanol for 30 min at room temperature. After a 30-min blocking step with horse serum, sections were incubated with 1:50 dilution of polyclonal rabbit anti-PAX2 antibody (Zymed Laboratories Inc., San Francisco, CA) overnight at 4 °C, followed by staining with the Vectastain ABC universal kit (Vector Laboratories, Burlingame, CA) as described by the manufacturer. Sections were then incubated with diaminobutyric acid reagent (Vector Laboratories). Sections were counterstained with Mayer's hematoxylin (Sigma) for 3 min, dehydrated, and mounted with Permount (Fisher).

Immunofluorescent staining was performed on 14-$\mu$m frozen sections of embryonic mouse kidney. Briefly, sections were rinsed in PBS for 10 min and fixed in ice-cold acetone for 10 min. Sections were blocked with horse serum for 1 h at room temperature and then incubated with a 1:50 dilution of primary polyclonal rabbit anti-PAX2 antibody (Zymed Laboratories Inc.) overnight at 4 °C. Sections were exposed for 1 h at room temperature to secondary anti-rabbit IgG (1:200) conjugated with Texas Red as per the manufacturer's recommendations (Vector Laboratories). Sections were then stained with a 1:200 dilution of fluorescein-labeled *Lotus tetragonolobus* lectin (Vector Laboratories) overnight at 4 °C and mounted with aqueous gel mount (Sigma).

To confirm the proximal tubule origin of JTC12 cells, monolayers were cultured on chamber slides in Dulbecco's modified Eagle's medium (Invitrogen) supplemented with 10% serum and 1% penicillin/streptomycin (Invitrogen) until they reached 60% confluence. The cells were fixed for 10 min on ice in 4% paraformaldehyde. After several washes in PBS, cells were incubated with fluorescein-labeled *L. tetragonolobus* lectin (Vector Laboratories) for 30 min at 37 °C. Slides were then rinsed in PBS and mounted with aqueous gel mount (Sigma).

*In Situ Hybridization*—Mouse *Wnt4* cDNA (851–1275 bp) subcloned into PGEM7zf vector was kindly provided by Dr. McMahon (Harvard University). The *Wnt4* antisense and sense probes (424 bp) were generated by linearizing the vector with BamHI and XbaI restriction endonucleases and Sp6 and T7 promoters, respectively. 0.5 $\mu$g (1 $\mu$l) of the plasmid template was combined with 125 $\mu$Ci of $^{35}$S-labeled $\alpha$-UTP (1320 Ci/mmol; PerkinElmer Life Sciences), 1 $\mu$l of 10× transcription buffer (100 mM NaCl, 400 mM Tris, pH 7.5, 60 mM MgCl$_2$, 100 mM DTT, 40 mM spermidine), 1.5 $\mu$l of 3.3 mM of ATP, GTP, and CTP mixture (Amersham Biosciences), 1 $\mu$l of 100 mM DTT, and 0.25 units of RNAguard (Roche Applied Science). 20 units of the appropriate enzyme was added, and the final mixture was incubated for 1 h at 37 °C. DNA template was digested with 2.5 units of DNase (Roche Applied Science) at 37 °C for 15 min. The cRNA probes were purified by ethanol precipitation in the presence of carrier yeast RNA and washed two times with 70% EtOH. Integrity of probe was checked on a 4% denaturing gel. $5 \times 10^4$ cpm/$\mu$l of the hybridization buffer in a volume of 100 $\mu$l was used for *in situ* hybridization on each slide.

E14.5 *Pax2*$^{1Neu}$ wild type and heterozygous mouse embryos were fixed in 4% paraformaldehyde and embedded in paraffin. Five-micron sections were mounted on Frost-Plus glass slides (Fisher), deparaffinized, rehydrated, and incubated with 5 $\mu$g/ml of proteinase K followed by three rinses in PBS. Slides were incubated for 2–4 h at room temperature in 100 $\mu$l of prehybridization buffer (4× SET, 1× Denhardt's, 0.5 mg/ml salmon sperm DNA, 0,6 mg/ml yeast RNA) mixed with 50% formamide followed by overnight incubation at 52.5 °C in 100 $\mu$l of 50% formamide and 1× hybridization buffer (4× SET, 1× Denhardt's solution, 100 $\mu$g/ml single-stranded DNA, 100 $\mu$g/ml yeast RNA, 10% dextran sulfate) combined with the labeled probe. Slides were washed twice in 2× SSC, 5 mM DTT at room temperature for 10 min and twice in the same buffer at 50 °C followed by two washes in 50% formamide, 1× SSC, 10 mM DTT at 55 °C and then at 62 °C. Slides were rinsed three times for 10 min in 0.5× SSC at room temperature and treated with 20 $\mu$g/ml RNase A in 3.5× SSC at 37 °C. They were then rinsed four times in 3.5× SSC and three times at room temperature in 2× SSC, followed by dehydration in ethanol. Slides were dipped in the photographic emulsion, exposed, counterstained with hematoxylin-eosin, and photographed.

*Electrophoretic Mobility Shift Assays (EMSAs)*—Probes for EMSAs were prepared from synthetically generated oligonucleotides. The sequences of the probes are as below. Putative sense (A and B) and antisense (C) core recognition nucleotides are double-underlined. Mutations were created in conserved core PAX2 recognition nucleo-

tides for sites A, B, and C; these are shown in boldface. For A, 5′-TCG-GCG**G**CGCGCAGC**CAG**GC**G**TGCCTGGAG-3′; for B, 5′-AGA**G**C-CCCCCG**T**CA**C**T**C**TTGA**AAACATCCT-3′; and for C, 5′-CAGT-ACGTACTTCCTAGATTTGTTGCA**AC**G**A**TTGA**ATGA-3′; for A (mut), 5′-TCGGCG**G**CGCG**A**AGC**CAG**GC**G**TGCCTGGAG-3′; for B (mut), 5′-AGA**G**CCCCCCG**TAA**CT**C**TT**TA**AAACATCCT-3′; and for C (mut), 5′-CAGTACGTAC**TTCC**TAGATTTGTTG**A**A**AC**GAT-**TTA**ATGA-3′. Synthetic oligonucleotide probes to the *WNT4* promoter region were labeled by back filling with the Klenow fragment of DNA polymerase I using [$\alpha$-$^{32}$P]dCTP (3000 Ci/mmol; PerkinElmer Life Sciences). The Pax2 proteins were synthesized using a T7-coupled transcription/translation reticulocyte lysate system (Promega). The *in vitro* translated products were incubated with $^{32}$P-labeled probes at room temperature for 15 min in a solution containing 4% Ficoll, 1 mM EDTA, pH 8.0, 10 mM HEPES, pH 7.9, 1 mM dithiothreitol (DTT), and 1 $\mu$g of poly[(dIdC)(dIdC)]. In some reactions, the protein was also preincubated with the 1 $\mu$g of anti-PAX-2/5/8(N-19) antibody (catalog number sc-7747; Santa Cruz Biotechnology) for 20 min at room temperature and then incubated with the radiolabeled probe for 20 min at room temperature. For competition experiments, reaction mixtures were preincubated for 15 min at room temperature with unlabeled oligonucleotide prior to the addition of radiolabeled probes. Following the binding step, reaction mixtures were electrophoresed on a 6% polyacrylamide gel (acrylamide/bisacrylamide ratio, 29:1) in 0.25× TBE buffer (22.25 mM Tris·HCl, 22.25 mM boric acid, and 1 mM EDTA) at 90 V at room temperature. The gels were dried and exposed to Kodak X-Omat film at room temperature.

*Stable Transfection of JTC12 Cells and Western Immunoblotting*—Subconfluent JTC12 cells were transfected with a *PAX2* expression vector, pCDNA3.1/*PAX2*, or with an empty vector without the *PAX2* insert, using the lipophilic transfection agent FuGENE™ 6 (Roche Applied Science). After 48 h, cells were then selected in medium containing 400 $\mu$g/ml G418 for 2–3 weeks; surviving colonies were pooled. Protein in whole cell extracts were resolved on 10% SDS-polyacrylamide gels, electroblotted onto Hybond ECL membrane (Amersham Biosciences), and probed with rabbit anti-PAX2 polyclonal antibody (1 $\mu$g/ml) (catalog number 71-6000, Zymed Laboratories Inc.), followed by incubation with horseradish peroxidase-conjugated goat anti-rabbit IgG (1:10,000; Bio-Rad). To visualize protein bands, blots were incubated in Western Lightning Chemiluminescence Reagent Plus according to the manufacturer's instructions (PerkinElmer Life Sciences) and exposed to Kodak X-Omat film. Band intensity was quantified and normalized for GAPDH.

*RNA Isolation*—Three litters of E15.5 *Pax2$^{1Neu}$* mice were sacrificed, and total RNA was extracted from each pair of kidneys. Genotypes of the *Pax2$^{1Neu}$* pups and their wild type littermates were identified as described previously (Clark Electromedical Instruments). Total RNA was isolated from kidney lysates with RNeasy columns (Qiagen, Valencia, CA) according to the manufacturer's directions. RNA was treated with DNase while bound to the RNeasy column.

*Real Time RT-PCR*—All real time RT-PCRs were carried out using the Mx4000 Multiplex Quantitative PCR System (Stratagene). We used the Qiagen QuantiTect™ SYBR® Green RT-PCR method for quantitative, real time one-step RT-PCR. Following reverse transcription with universal primers, PCR amplifications were performed using the recommended buffer supplied by the manufacturer. Primers included the following: 5′*Wnt4*(sense), ACCTGGAAGTCATGGACTCG; 3′*Wnt4*-(antisense), TCAGAGCATCCTGACCACTG. Each 25-$\mu$l PCR contained cDNA, forward and reverse primers, and the passive reference dye (ROX) to normalize the SYBR Green/double-stranded DNA complex
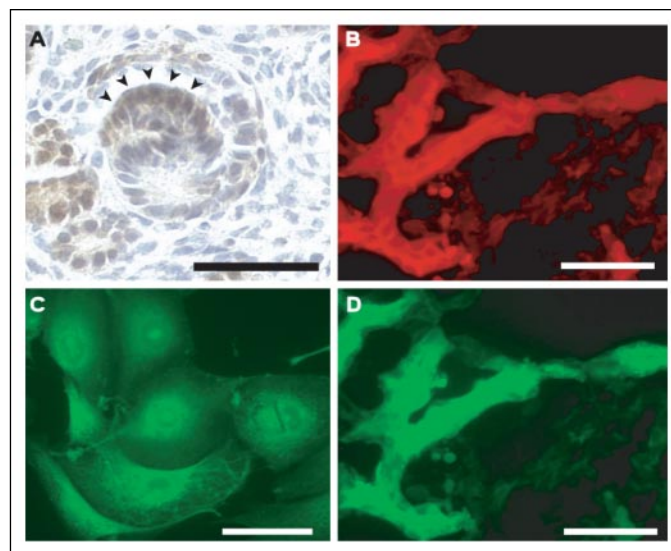


FIGURE 1. **PAX2 protein expression in fetal mouse kidney.** *A,* PAX2 protein was identified by immunohistochemistry in the distal portion of the S-shaped bodies (*arrowheads*) of E15.5 fetal mouse kidneys. *B,* in frozen sections of E16.5 fetal mouse kidney, PAX2 protein was evident in epithelial cells of developing tubules. Anti-PAX2 antibody was detected by immunofluorescent staining with Texas Red-labeled second antibody. *C,* simian JTC12 cells are derived from proximal tubules and exhibit staining for the fluorescein-tagged proximal tubule marker, *L. tetragonolobus* lectin as do the PAX2-positive cells of fetal mouse kidney (*D*).

signal during analysis to correct for well-to-well variations. Triplicate or quadruplicate reactions were performed for each template amount. DNA standard template was replaced with water in all no-template controls. We performed simultaneous real time RT-PCR with glyceraldehyde-3-phosphate dehydrogenase (*Gapdh*). All *N*-methyl-D-aspartic acid values were normalized for *Gapdh*. PCR cycling conditions were as follows: initial denaturation at 95 °C for 15 min according to manufacturer's recommendations, followed by 35 cycles of 94 °C for 1 min, 1 min of annealing (annealing temperature adapted for specific primer set used), and 1 min/kb extension at 72 °C. The identities of the PCR products were examined by melting curve analysis on the Mx4000 and by agarose gel electrophoresis. Data analysis was performed using the Mx4000 software. The calculated threshold (*CT*) was determined for all samples and defined as the amount of the *Wnt4* gene in relation to the reference gene *Gapdh*. All results are displayed as fold induction of target gene mRNA expression as determined by the $\Delta CT$ method. Briefly, $\Delta CT$ indicates the difference between the number of cycles necessary to detect the PCR products of *Wnt4* and the reference gene *Gapdh*.

## RESULTS

*PAX2 Is Expressed in the Distal S-shaped Body and Persists in Fetal Proximal Tubule*—Previous investigators have demonstrated *Pax2* mRNA expression in induced mesenchymal cells as they cluster at the tip of each ureteric bud branch (2). Our immunohistochemical studies show that PAX2 protein expression is sustained in tubular cells of the distal loop of S-shaped bodies (Fig. 1*A*). However, PAX2 protein is conspicuously absent in epithelial cells at the proximal loop of the S-shaped body, which will give rise to podocytes of the primitive glomerulus (Fig. 1*A*). PAX2 expression is evident in maturing tubules that stain for the differentiated proximal tubule marker, *L. tetragonolobus* lectin (Fig. 1, *B–D*). The JTC12 cell line, derived from simian renal proximal tubule, also exhibits immunofluorescent staining for *L. tetragonolobus* lectin (Fig. 1*C*) and was used for the *in vitro* studies of PAX2 and *WNT4* below.

*PAX2 Activates the WNT4 Promoter in Vitro*—To determine whether PAX2 activates *WNT4* promoter activity *in vitro*, a 10.7-kb 5′-flanking sequence of the human *WNT4* gene (15) was cloned into a luciferase reporter vector and co-transfected with a full-length human *PAX2b* expression vector into cultured JTC12 cells (Fig. 2). Luciferase activity in cell extracts was assayed after 48 h. In the presence of PAX2b,
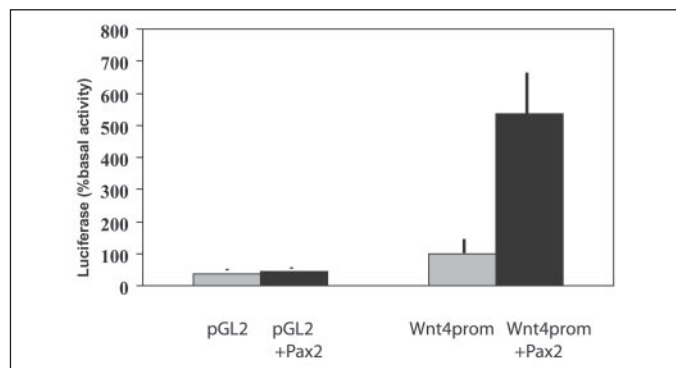


FIGURE 2. **PAX2 activates transcriptional activity of the human *WNT4* promoter.** JTC12 cells were transiently co-transfected with a pGL2 luciferase reporter vector driven by a 10.7-kb fragment of the human *WNT4* gene 5′-flanking sequence and a mammalian expression vector containing the full-length human *PAX2* cDNA. Luciferase activity was assayed after 48 h and expressed as a percent of basal promoter activity. Empty pGL2 vector luciferase activity was one-third of that in the presence of a *WNT4* promoter. In the presence of exogenous PAX2, basal promoter activity was stimulated 5.4-fold.

transcriptional activity of the 10.7-kb *WNT4* promoter was increased 5-fold.

*Description of Putative PAX2-binding Sites in the WNT4 Promoter*—To determine whether the *WNT4* promoter contains plausible PAX2-binding sites, we screened the 10.7-kb 5′-flanking sequence of the human *WNT4* gene (15) with MatInspector software. The recognition motif for PAX2 has been studied by others and appears to vary significantly from gene target to gene target. Nevertheless, a consensus sequence consisting of about 11 core nucleotides spaced over a stretch of 25 bp has been proposed (4). Of 11 putative sites with partial homology to this consensus sequence, only 5 were subsequently shown to specifically bind PAX2 protein. The first putative PAX2-binding motif (motif A in Fig. 3A) was identified close (−461 to −435 in sense orientation) to the transcriptional start site. It contained only 7 of the 11 core nucleotides of the PAX2 consensus sequence but was selected for study because it also exhibited homology with the "PAX5" recognition sites.

A second (motif B1 at −2428 to −2405) and third (motif C1 at −2460 to −2581) putative PAX2 recognition sequence were identified further upstream, positioned fairly closely together and in sense and antisense orientations, respectively. These two motifs contained 9 (motif B1) and 6 (motif C1) nucleotides of the PAX2 consensus sequence, respectively.

Most interestingly, motifs C1 and B1 lie within a 0.66-kb cassette of DNA (−5331 to −4672) that was completely duplicated further



FIGURE 3. **Putative PAX2-binding sites in the human *WNT4* promoter.** *A* and *B,* the 10.6-kb 5′-flanking sequence of the human *WNT4* gene was analyzed with MatInspector software for possible PAX2-binding motifs. Three of 11 potential PAX2 recognition motifs were subsequently shown to bind PAX2 protein in gel shift assays. Two motifs (*B1* and *C1*) lie within a 660-bp cassette duplicated further upstream. *C,* the three putative unique PAX2-binding motifs are compared with other published sequences.
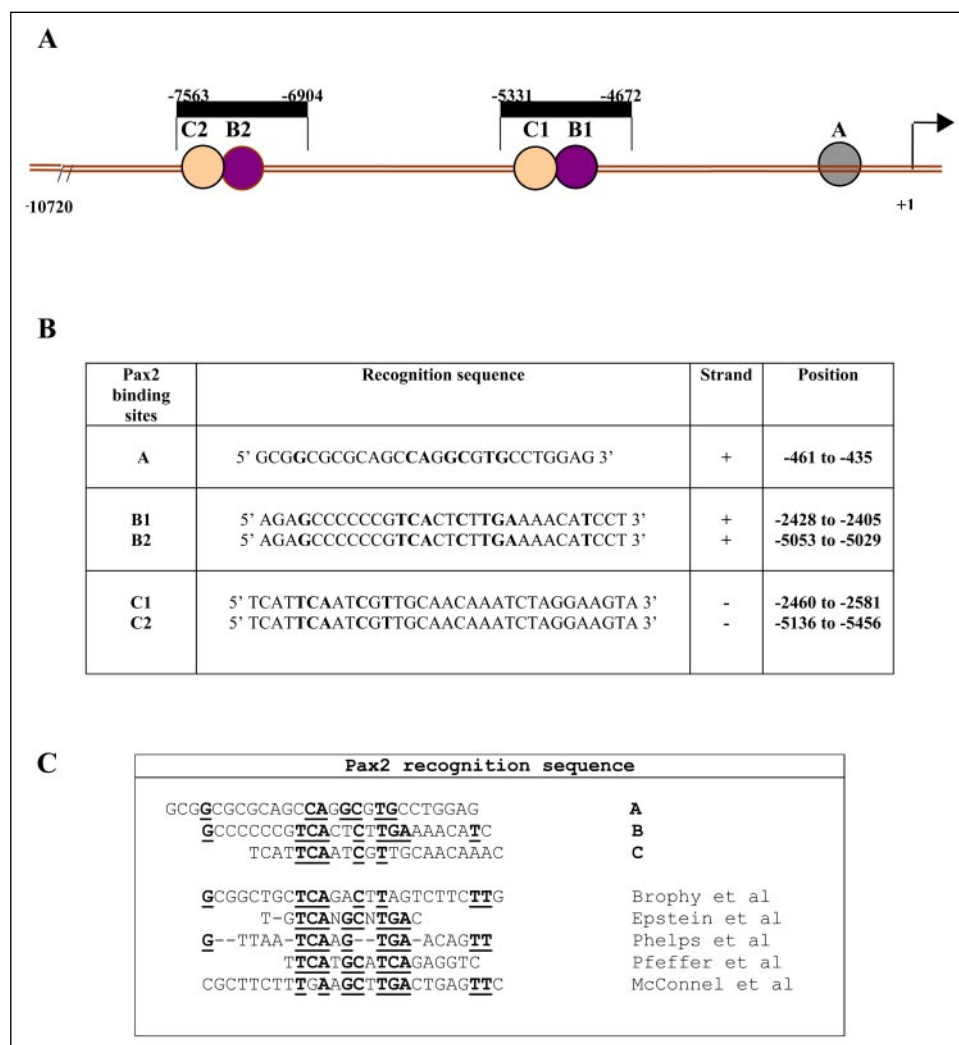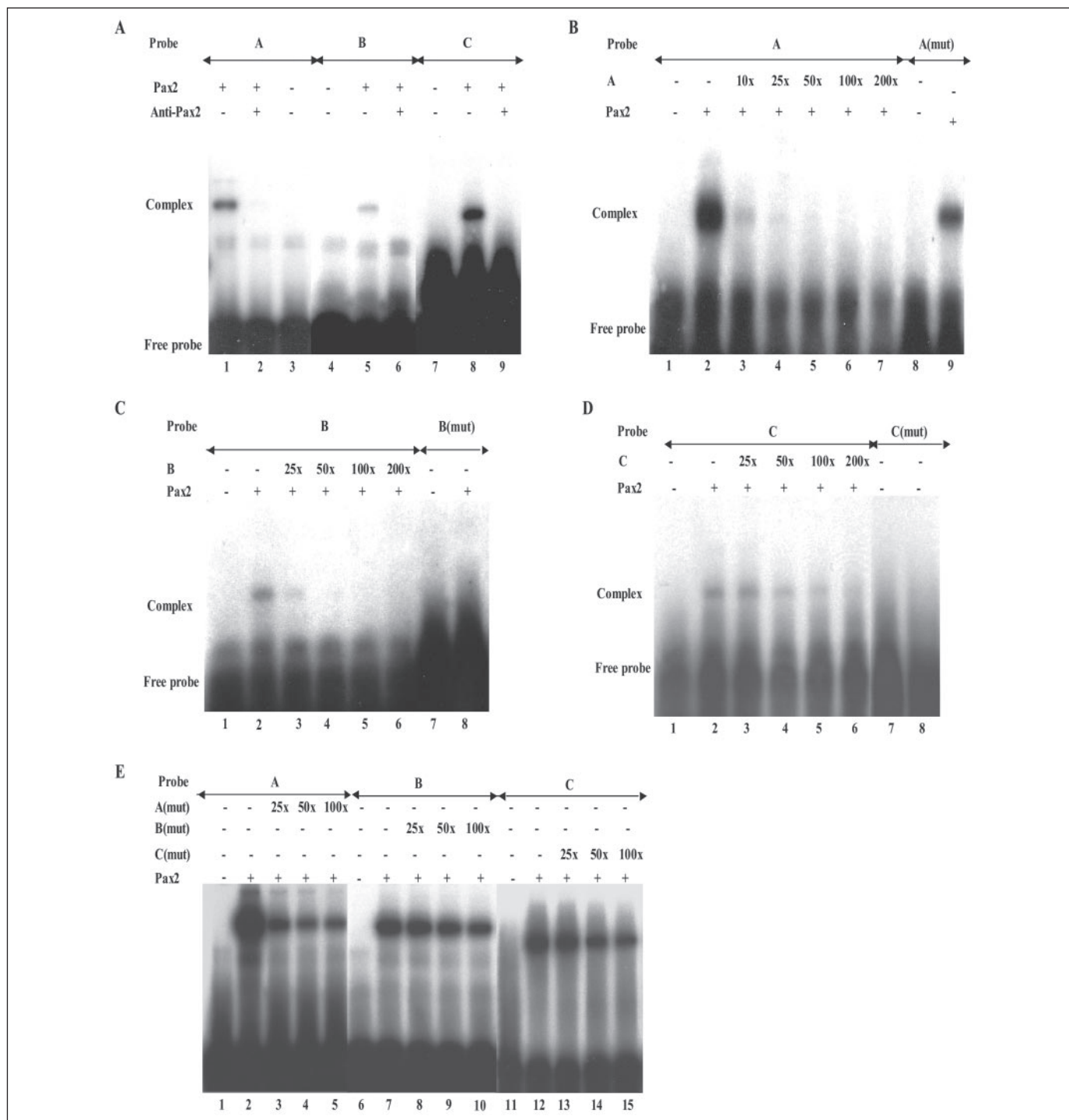
FIGURE 4. **Electrophoretic mobility shift assays for PAX2 binding to putative recognition motifs in the *WNT4* promoter.** *A,* PAX2 protein forms a unique complex with radiolabeled probe A (*lane 1*), probe B (*lane 5*), or probe C (*lane 8*) that disappear in the presence of anti-PAX2 antibody (*lanes 2, 6,* and *9,* respectively). *B,* the radiolabeled PAX2-probe A complex is competed out by progressively increasing amounts of cold unlabeled probe A (*lanes 2–7*). Mutation of a single cytosine to an adenine within the putative PAX2 recognition motif significantly diminishes the PAX2-probe band (*lanes 8* and *9*). *C,* the radiolabeled PAX2-probe B complex is competed out by increasing amounts of unlabeled probe B (*lanes 2–7*). For the mutation of two core nucleotides of the putative PAX2 recognition motif in probe B, no complex formation is seen (*lane 8*). *D,* the radiolabeled PAX2-Probe C complex is competed out by increasing amounts of unlabeled probe C (*lanes 2–6*). Mutation of two core nucleotides in probe C eliminates complex formation (*lane 8*). *E,* although complex inhibition by unlabeled wild type oligonucleotides was evident at 25-fold excess (probe A), 50-fold excess (probe B), and 100-fold excess (probe C) (*lane 4* (*B*), *lane 4* (*C*), and *lane 5* (*D*), respectively), mutant unlabeled oligonucleotides were ineffective competitors at similar molar ranges. Protein-DNA complexes were resolved on nondenaturing 6% polyacrylamide gels electrophoresed at room temperature in 0.25× TBE. Complexes were visualized by drying the gel and exposing to film (Eastman Kodak Co.) at room temperature. The positions of free probe and protein-DNA complexes are indicated.

upstream (−7563 to −6904) (Fig. 3*A*). Thus, two additional putative PAX2 motifs (B2 and C2) were identified close together lying on opposite DNA strands, but these were duplicates of sites in the downstream cassette. The three unique putative PAX2-binding motifs and sur-

rounding nucleotide sequences are listed in Fig. 3*B* and compared with PAX2 recognition motifs reported by others (Fig. 3*C*).

*EMSA*—To determine whether the three putative recognition motifs exhibited specific high affinity PAX2 binding, a series of gel shift experi-
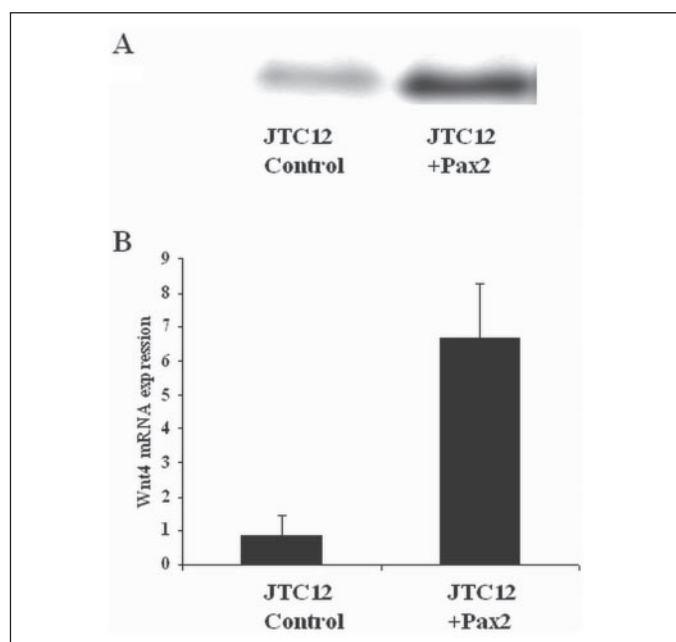
FIGURE 5. *A,* monkey kidney proximal tubular cell line (JTC12) was stably transfected with human *PAX2* cDNA, increasing PAX2 protein expression above the modest endogenous level. *B,* up-regulation of *WNT4* mRNA in JTC12 cells overexpressing PAX2 was confirmed by quantitative real time RT-PCR and normalized for *Gapdh* mRNA.
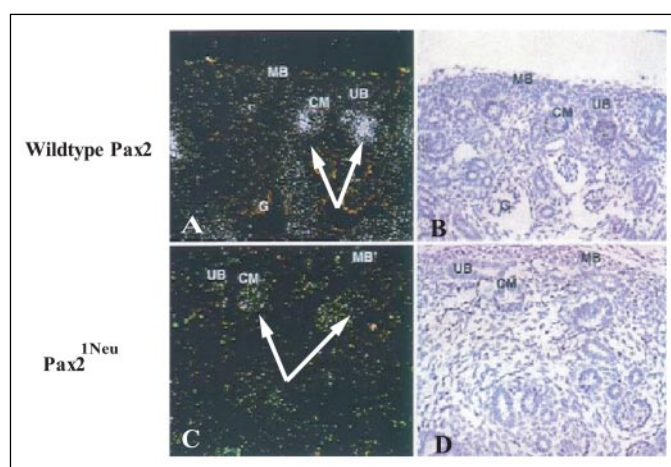


FIGURE 6. *In situ* hybridization analysis of *Wnt4* expression in fetal wild type and heterozygous *Pax2^{1Neu}* kidneys. Sections of E15 wild type and *Pax2^{1Neu}* mutant embryos were hybridized to a murine *Wnt4* riboprobe. *B* and *D,* bright field. *A* and *C,* dark field. Magnification ×200. Condensing mesenchyme (*CM*) shows intense silver grain deposition in wild type kidney (*A* and *B*) but not in heterozygous mutant kidneys (*C* and *D*). Metanephric blastema (*MB*), ureteric bud (*UB*), and glomeruli (*G*) are negative for *Wnt4* expression in both wild type and *Pax2^{1Neu}* kidneys.

ments was performed with radiolabeled oligonucleotides containing the A–C sequences and *in vitro* translated PAX2 protein. Incubation of PAX2 protein with each radiolabeled probe resulted in single protein-DNA complexes seen as band shifts in Fig. 4*A, lanes 1, 5,* and *8*. The complex disappeared in the presence of PAX2 antibody (Fig. 4*A, lanes 2, 6,* and *9*) but not nonimmune serum (data not shown). The specificity of Pax2 binding was examined in competition assays with increasing amounts of excess unlabeled wild type oligonucleotides A–C (Fig. 4, *B–D*) and mutant oligonucleotides A (mut), B (mut), and C (mut) (Fig. 4*E*). Binding of PAX2 to probes A–C was competed out by increasing amounts of unlabeled wild type oligonucleotides A–C (Fig. 4, *B–D*). Competition was evident at 25-fold excess (probe A), 50-fold excess (probe B), and 100-fold excess (probe C) unlabeled wild type oligonucleotide. EMSAs were also performed with PAX2 protein and mutated oligonucleotides A (mut), B (mut), and C (mut), as probes. Mutation of a single core nucleotide in the putative recognition motif of probe A significantly reduces complex band intensity (Fig. 4*B, lanes 9 versus 2*). When core nucleotides of motif B and C were mutated, complex formation was completely abrogated (Fig. 4, *C, lanes 8 versus 2,* and *D, lanes 8 versus 2*). Similarly, mutant cold oligonucleotides were unable to inhibit complex formation in the same molar range as the unlabeled wild type oligonucleotide competitors (Fig. 4*E*). Thus, PAX2 recognizes each of the three sites in sequence-specific fashion.

*PAX2 Activates Endogenous WNT4 in JTC12 Cells*—JTC12 cells are derived from the monkey proximal tubule lineage and express the proximal tubular marker, *L. tetragonolobus* lectin. The cells express modest levels of endogenous PAX2, identifiable by Western immunoblotting (Fig. 5*A*). To examine the effect of PAX2 on endogenous WNT4 expression, JTC12 cells were stably transfected with a cytomegalovirus-driven human *PAX2* expression vector and selected in neomycin-containing culture medium. Stable transfectants were isolated and re-assessed for PAX2 protein level by Western immunoblotting. As seen in Fig. 5*A*, the JTC12/*PAX2* stable transfectants expressed about five times as much PAX2 protein as the parent cell line.

Endogenous *WNT4* mRNA levels were measured in control (parent) JTC12 cells and in the stable JTC12/*PAX2* transfectants by real time

RT-PCR, normalizing samples for *Gapdh* mRNA amount. As seen in Fig. 5*B*, *WNT4* mRNA levels were about 7-fold higher in the JTC12/*PAX2* transfectants compared with control cells.

*WNT4 Expression Is Reduced in the Pax2^{1Neu} Mutant Mouse*—In previous studies we demonstrated that fetal kidneys from *Pax2^{1Neu}* heterozygotes have reduced PAX2 protein and moderately severe renal hypoplasia, although the architecture of individual nephrons is relatively normal (6). To determine whether the *in vitro* evidence of *WNT4* regulation by PAX2 reflects an important molecular pathway for mammalian kidney development *in vivo*, we assessed endogenous *Wnt4* expression in E15 fetal kidney of heterozygous *Pax2^{1Neu}* mutant mice and their wild type littermates. Heterozygous male *Pax2^{1Neu}* C3H mice were crossed with wild type C3H females. E15 embryos were genotyped as described previously (8), and fetal kidneys were isolated and processed for *in situ* hybridization studies with a *Wnt4* riboprobe. As seen in Fig. 6, *A* and *B*, *Wnt4* mRNA expression is abundant but is highly restricted to the condensing mesenchyme adjacent to ureteric bud branch tips (*arrows*) in normal fetal kidney. In contrast, the *Wnt4* signal is barely detectable in condensing mesenchyme of *Pax2^{1Neu}* fetal kidneys (Fig. 6, *C* and *D*). Similarly, *in situ* hybridization studies were performed for *Eya1*, another transcription factor expressed in early induced renal mesenchyme; *Eya1* mRNA expression was comparable in *Pax2^{1Neu}* and wild type E15.5 kidneys (data not shown).

*Wnt4* mRNA was quantified in mutant and wild type fetal kidneys by real time RT-PCR and normalized for *Gapdh* mRNA in the same samples. In keeping with our *in situ* hybridization studies, relative *Wnt4* mRNA in E15.5 *Pax2^{1Neu}* mutant kidney was only 40% of that in kidneys from wild type littermates (Fig. 7).

## DISCUSSION

*Potential Functions of the PAX2/WNT4 Pathway during Nephrogenesis*—PAX2 plays a central role in the caudal descent of the nephric duct, the emergence of ureteric buds, and the subsequent branching morphogenesis of the collecting system. *PAX2* mRNA is also abundant in metanephric mesenchymal cells as they cluster at UB tips (2), and its function there is as yet unknown. Our immunohistochemical studies show that PAX2 protein expression is sustained beyond this stage. It appears in distal portions of the developing S-shaped body as
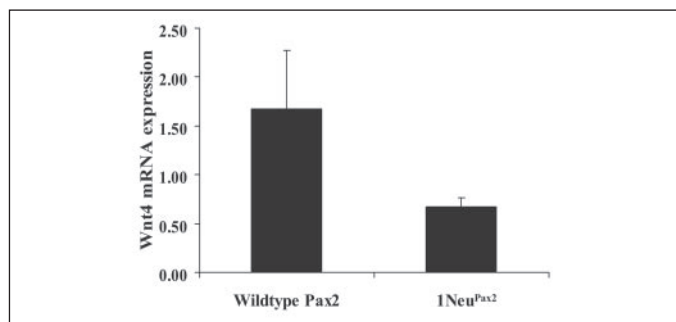
**FIGURE 7. Real time RT-PCR estimation of *Wnt4* mRNA normalized for *Gapdh* mRNA in the same samples from wild type E15.** Five fetal mouse kidney and heterozygous *Pax2$^{1Neu}$* littermates are shown.

differentiation proceeds and is still evident in the early fetal proximal tubule. Apparently, PAX2 is involved both in the process whereby metanephric mesenchyme is transformed into polarized epithelium and/or in the maturation of the proximal convoluted tubule as it undergoes terminal differentiation.

Previous reports suggest that these events are also critically dependent on expression of the secreted growth factor, WNT4. In mice with homozygous inactivation of the *Wnt4* gene, the UB successfully contacts metanephric mesenchyme and induces mesenchymal cells to cluster and express PAX2 at its tips (10, 17). However, subsequent progression to the S-shaped body stage does not occur (10, 17). This observation places PAX2 temporally upstream of WNT4 during this process. Our studies demonstrate reduced *Wnt4* mRNA in the *Pax2$^{1Neu}$* mouse and indicate that Pax2 is functionally upstream of WNT4 expression in the developmental cascade as well.

There is some evidence that WNT4 is involved in cell movement during development. Acting through the frizzled3 receptor, WNT4 guides murine commissural axons as they cross the midline (18). In *Drosophila*, WNT4 has been implicated in cell movements requiring disassembly of focal adhesion complexes; *Drosophila* WNT4 regulates focal adhesion kinase during ovarian morphogenesis through the noncanonical protein kinase C pathway (19). Conceivably, WNT4 signaling via this pathway might play a role in the spectacular serpentine growth of the S-shaped body and proximal convoluted tubule.

On the other hand, there is also evidence that WNT4 may have a set of effects mediated through the canonical $\beta$-catenin signaling pathway (13). This intracellular pathway responds to WNT activation of heterodimeric frizzled/LRP6 receptors at the surface of target cells (20). Activated canonical receptors recruit DSH and other partners to suppress degradation of $\beta$-catenin and facilitate its transfer to the nucleus. There, $\beta$-catenin combines with transcription factor partners of the TCF/LEF family to regulate expression of target genes (21). Rod cell production in the developing retina is promoted by canonical WNT4/FZD4/LRP6 signaling (22). Canonical WNT4 signaling drives synovial joint development (23) and mediates the effects of estrogen on uterine growth (24).

High levels of canonical $\beta$-catenin signaling activity have been identified in both the distal S-shaped body and tips of the ureteric bud during mouse kidney development (25, 26). Thus, PAX2-activated WNT4 expression might drive autocrine canonical signaling during formation of the S-shaped body. There is the interesting possibility that WNT4 could also provide a paracrine signal to the adjacent ureteric bud tip. WNT4 is reported to activate the canonical $\beta$-catenin signaling pathway in cultured Madin-Darby canine kidney cells derived from the canine UB lineage (13). WNT4 has been implicated in side-branching of mammary ductal cells during breast development (27). *Wnt4* knock-out

mouse fail to form S-shaped bodies, but this is accompanied by an abrupt halt to any further UB branching (10).

*PAX2 Binding to Novel Motifs within the WNT4 Gene Promoter*—We demonstrate that PAX2 directly activates transcriptional activity of the 5′-flanking sequence of the human *WNT4* gene, containing several unique PAX2 recognition motifs. A novel 26-bp sequence (labeled *motif A* in Fig. 1*A*) about 0.45 kb upstream of the transcriptional start site showed homology both to the consensus PAX2 recognition motif proposed by Brophy *et al.* (4) and to the PAX5 motif used in MatInspector software. *Pax2, -5,* and *-8* form a subgroup within the *Pax* gene family based on domain structure; crossover between PAX2 and PAX5 binding sequences has been noted in other gene targets (16). Two other motifs within the 5′-flanking sequence of the human *WNT4* gene (*labeled motifs B* and *C* in Fig. 1*A*) were more similar to the published PAX2 consensus recognition motif (4). Most interestingly, PAX2-binding motifs $B_1$ and $C_1$ were located in close proximity to each other oriented on opposite (sense and antisense) DNA strands and lie within a 0.66-kb cassette ($-5331$ to $-4672$) that was completely duplicated at an upstream site ($-7563$ to $6904$) in the 5′-flanking sequence. Possibly, this duplication event reflects the importance of these PAX2 motifs and/or other elements of the cassette in regulating WNT4 expression.

It is unclear why the *WNT4* gene should contain several slightly different recognition motifs for PAX2, yet each of the motifs (A, $B_1/B_2$, or $C_1/C_2$) exhibited specific high affinity binding to PAX2 protein in EMSAs. In each case, the PAX2-probe complex was sensitive to anti-PAX2 antibody, mutation of core PAX2 recognition motif base pairs, and addition of cold-unlabeled motif DNA. Clearly, other transcription factors could be involved in determining the highly restricted expression of WNT4 in mesenchymally derived portions of the renal tubule; PAX2 is expressed at other sites in the developing kidney (*e.g.* ureteric bud) where WNT4 expression is absent. Presumably, additional transcription factors are required to achieve a combinatorial specificity with PAX2 and account for the highly restricted pattern of WNT4 expression. The variability of PAX2 recognition sequences might reflect the molecular complexity of this regulation.

*PAX2 Activates Endogenous WNT4 Gene in Vivo*—The *in vitro* interactions between PAX2 and the *WNT4* promoter are clearly relevant during *in vivo* renal development. Endogenous *Wnt4* mRNA expression was significantly reduced in the mesenchymal condensates/S-shaped bodies of heterozygous mutant *Pax2$^{1Neu}$* mouse fetal kidneys. Interestingly, heterozygous mutant *Pax2$^{1Neu}$* fetal mouse kidneys are hypoplastic (6), but the reduction in WNT4 expression is not sufficient to prevent formation of some normal appearing S-shaped bodies during development. This is not surprising, however, because normal appearing S-shaped bodies were also noted in fetal kidneys of heterozygous *Wnt4* knock-out mice. Thus, the developmental cascade allowing differentiation of S-shaped bodies seems to require only a modest level of PAX2 and WNT4. Below some minimal threshold, however (as in homozygous *Wnt4* knock-out mice), S-shaped body formation does not occur.

*Conclusion*—During renal development, PAX2 is expressed in the distal portion of the emerging S-shaped body and early proximal tubule. We suggest that it binds directly to novel response elements in the *WNT4* promoter, activating transcription during the mesenchyme to epithelium transition. WNT4 expression continues in the S-shaped body and early proximal tubule and could influence its serpentine growth and terminal differentiation. Conceivably, PAX2 activation of *WNT4* could initiate a paracrine feedback signal to ureteric bud cells and promote further rounds of branching nephrogenesis.

## REFERENCES

1. Dressler, G. R., Deutsch, U., Chowdhury, K., Nornes, H. O., and Gruss, P. (1990) *Development* (*Camb.*) **109,** 787–795
2. Torres, M., Gomez-Pardo, E., Dressler, G. R., and Gruss, P. (1995) *Development* (*Camb.*) **121,** 4057–4065
3. Bouchard, M., Souabni, A., Mandler, M., Neubuser, A., and Busslinger, M. (2002) *Genes Dev.* **16,** 2958–2970
4. Brophy, P. D., Ostrom, L., Lang, K. M., and Dressler, G. R. (2001) *Development* (*Camb.*) **128,** 4747–4756
5. Torban, E., Eccles, M. R., Favor, J., and Goodyer, P. R. (2000) *Am. J. Pathol.* **157,** 833–842
6. Porteous, S., Torban, E., Cho, N. P., Cunliffe, H., Chua, L., McNoe, L., Ward, T., Souza, C., Gus, P., Giugliani, R., Sato, T., Yun, K., Favor, J., Sicotte, M., Goodyer, P., and Eccles, M. (2000) *Hum. Mol. Genet.* **9,** 1–11
7. Dziarmaga, A., Clark, P., Stayner, C., Julien, J. P., Torban, E., Goodyer, P., and Eccles, M. (2003) *J. Am. Soc. Nephrol.* **14,** 2767–2774
8. Clark, P., Dziarmaga, A., Eccles, M., and Goodyer, P. (2004) *J. Am. Soc. Nephrol.* **15,** 299–305
9. Torban, E., and Goodyer, P. R. (1998) *Biochim. Biophys. Acta* **1401,** 53–62
10. Stark, K., Vainio, S., Vassileva, G., and McMahon, A. P. (1994) *Nature* **372,** 679–683
11. Kispert, A., Vainio, S., and McMahon, A. P. (1998) *Development* (*Camb.*) **125,** 4225–4234
12. Huelsken, J., and Birchmeier, W. (2001) *Curr. Opin. Genet. Dev.* **11,** 547–553
13. Lyons, J. P., Mueller, U. W., Ji, H., Everett, C., Fang, X., Hsieh, J. C., Barth, A. M., and McCrea, P. D. (2004) *Exp. Cell Res.* **298,** 369–387
14. Stayner, C. K., Cunliffe, H. E., Ward, T. A., and Eccles, M. R. (1998) *J. Biol. Chem.* **273,** 25472–25479
15. Sim, E. U., Smith, A., Szilagi, E., Rae, F., Ioannou, P., Lindsay, M. H., and Little, M. H. (2002) *Oncogene* **21,** 2948–2960
16. Wheat, W., Fitzsimmons, D., Lennox, H., Krautkramer, S. R., Gentile, L. N., McIntosh, L. P., and Hagman, J. (1999) *Mol. Cell. Biol.* **19,** 2231–2241
17. Kispert, A., Vainio, S., Shen, L., Rowitch, D. H., and McMahon, A. P. (1996) *Development* (*Camb.*) **122,** 3627–3637
18. Lyuksyutova, A. I., Lu, C. C., Milanesio, N., King, L. A., Guo, N., Wang, Y., Nathans, J., Tessier-Lavigne, M., and Zou, Y. (2003) *Science* **302,** 1984–1988
19. Cohen, E. D., Mariol, M. C., Wallace, R. M., Weyers, J., Kamberov, Y. G., Pradel, J., and Wilder, E. L. (2002) *Dev. Cell* **2,** 437–448
20. He, X., Semenov, M., Tamai, K., and Zeng, X. (2004) *Development* (*Camb.*) **131,** 1663–1677
21. Nusse, R. (2005) *Cell Res.* **15,** 28–32
22. Hunter, D. D., Zhang, M., Ferguson, J. W., Koch, M., and Brunken, W. J. (2004) *Mol. Cell. Neurosci.* **27,** 477–488
23. Guo, X., Day, T. F., Jiang, X., Garrett-Beal, L., Topol, L., and Yang, Y. (2004) *Genes Dev.* **18,** 2404–2417
24. Hou, X., Tan, Y., Li, M., Dey, S. K., and Das, S. K. (2004) *Mol. Endocrinol.* **18,** 3035–3049
25. Maretto, S., Cordenonsi, M., Dupont, S., Braghetta, P., Broccoli, V., Hassan, A. B., Volpin, D., Bressan, G. M., and Piccolo, S. (2003) *Proc. Natl. Acad. Sci. U. S. A.* **100,** 3299–3304
26. Iglesias, D. M., Q. J., Chu, L. L., Othman, M., Dufort, and D., Goodyer, P. (2004) *J. Am. Soc. Nephrol.* **15,** 58A
27. Brisken, C., Heineman, A., Chavarria, T., Elenbaas, B., Tan, J., Dey, S. K., McMahon, J. A., McMahon, A. P., and Weinberg, R. A. (2000) *Genes Dev.* **14,** 650–654

# PAX2 Activates WNT4 Expression during Mammalian Kidney Development

Elena Torban, Alison Dziarmaga, Diana Iglesias, Lee Lee Chu, Tatiana Vassilieva,
Melissa Little, Michael Eccles, Maria Discenza, Jerry Pelletier and Paul Goodyer